J. Fluid Mech. (1967), *vol.* 28, *part* 3, *pp.* 439–462
Printed in Great Britain

Some new correlation measurements in a turbulent boundary layer

By D. J. TRITTON
School of Physics, University of Newcastle upon Tyne

(Received 10 January 1966 and in revised form 29 August 1966)

This paper presents some new velocity correlation measurements in a two-dimensional zero-pressure-gradient turbulent boundary layer; these extend the work of Grant (1958). The most detailed of the new measurements concern: correlations between velocity fluctuations in the mean flow direction and fluctuations perpendicular to the wall at a different point, usually but not always in the same plane parallel to the wall; correlations between velocity fluctuations in the mean flow direction and fluctuations perpendicular to this but parallel to the wall, usually but not always close to the wall with the separation in the same direction as the latter velocity fluctuation; and various correlations with a fixed separation normal to the wall and a simultaneous variable separation in the mean flow direction.

The results are not consistent with any of the various models of the large eddy structure that have been proposed. The features of the present work most relevant to the formulation of a substitute are brought together in §9. Included are suggestions that the similarities between the wall and outer regions are more marked than the differences, and that the description of the large eddies in the wall region as a coherent eruption from the viscous sublayer is unsatisfactory.

The new experiments are considered in connexion with three questions posed by the previous work. These concern the large eddy contribution to the Reynolds stress; the asymmetry between upstream and downstream separations when there is also a separation normal to the wall; and the similarity between boundary layers and channel flow. A complicated situation surrounds the first point; there are arguments suggesting that the large eddy contribution might in some places be of opposite sign to the total Reynolds stress, but this no longer seems so likely. The upstream–downstream asymmetry is also more complicated than had been previously supposed, but the results can be systematically interpreted if the peaks of the correlation curves are considered in connexion with continuity and the tails of the curves are considered in connexion with the shearing action of the mean flow. Regarding the third point, the present experiments give no indication of any difference in the large eddy structure in the wall regions of boundary layer turbulence and channel flow turbulence.

Section 5 gives a brief account of some experiments with a vibrating ribbon in the turbulent boundary layer.

1. Introduction

The main purpose of this paper is to present some new measurements of correlation functions in a turbulent boundary layer. These were made with particular questions in mind (see below), but seen in retrospect their chief importance is probably as one of several contributions towards a revised model of the large eddies. Previous models have been proposed by Grant (1958), Townsend (1957), Lilley & Hodgson (1960) and Lilley (1963), based primarily on Grant's measurements of the nine principal space correlation functions. There is now much more information available. Favre, Gaviglio and Dumas (1957, 1958) have made extensive measurements of space–time correlations, from which one would hope to be able to infer much about the development of the large-scale motions. Although these measurements are very detailed in their coverage of different separations in space and time, they are, on the other hand, restricted by being entirely of R_{11} correlations (see §2 for notation). Also relevant are the correlation measurements in channel flow by Comte-Bellot (1961*b*) and the flow visualization experiments of Kline & Runstadler (1959).

The present work adds further space-correlation measurements: a few of R_{11} and R_{22}; an extensive survey of R_{12}, particularly, but not only, with r_1-separation and r_3-separation; and some of R_{13}, particularly close to the wall with r_3-separation. The R_{11}, R_{22} and R_{12} measurements include a number of surveys with a fixed r_2-separation and a simultaneous variable r_1-separation.

Since much of the previous work mentioned above had not been incorporated into any description of the turbulence structure, it may seem to the reader that the present need is not further measurements but a deeper understanding of existing ones. Such indeed would be my own reaction on hearing of new measurements. However, there were certain questions about the structure of turbulent boundary layers which, it seemed to me, were posed but not answered by a study of the existing data. These concerned: the contribution of the large eddies to the Reynolds stress; the orientation of the large eddies, as suggested by upstream–downstream asymmetry of certain correlations; and the similarity (or lack of it) of the large eddies in the wall regions of boundary layer turbulence and channel turbulence.

Most of the measurements reported in §4 were made in the hope that they would give information relevant to one or other of these questions. Further indications of the reasoning behind the choice of measurements will be found in §§6–8, where the three issues are discussed as they now appear with my own results taken into account.

To comments on the choice of measurements should be added a reminder that what results are obtained using hot-wire anemometers depends to some extent on the course of events during the work. A substantial part of the time and effort for each configuration goes into the setting-up of the probes. Sometimes it then turns out that the results are unlikely to be satisfactory. Hence, when everything is running satisfactorily there is a temptation to obtain all the data one can. This should be resisted, but there may be some results that were obtained largely as the best way of occupying the half-hour till tea time! Conversely, there are a few

places where a little more data would have been desirable; the reason is usually that something went wrong (most often a wire breaking) towards the end of the run, and it did not seem worth while starting again for a few readings.

The survey, which raised the question above, of the available information on the large eddies was made as part of an investigation of the effect on these eddies of placing a vibrating ribbon in the boundary layer. This investigation was not very successful, but a brief account of it is given in §5.

Section 9 draws attention to the main implications of the present work for any new model of the large eddies. However, the development of one requires analysis of all the many relevant papers (see above) in conjunction, and this is not attempted in the present paper. At the time of writing, I have not succeeded in formulating a simple model of the large eddies (of the same general type as those proposed by Grant and Townsend) consistent with the present information. It may be that the true situation is too complicated for such simple models to work. On the other hand, the new results do give further support to the hypothesis (Townsend 1956) that the large eddies have a characteristic structure of their own. Hence, I am continuing to look for a useful model. In the meantime perhaps these new results may stimulate proposals from other people.†

2. Notation

The notation used to indicate the particular quantities measured is, with some variations in detail, that used by most previous authors; the principal exception is Favre, Gaviglio & Dumas, and, for comparison purposes, it is sometimes convenient to refer to their work as re-presented by Rotta (1962). Cartesian coordinates are taken with x as the distance in the mean flow direction downstream from the trip wire, y as the distance from the wall, and z parallel to the wall and normal to the mean flow. Components of the turbulent velocity fluctuation in the x-, y- and z-directions are denoted by u_1, u_2 and u_3 respectively. Components of the separation between two measuring stations a and b are correspondingly denoted by r_1, r_2 and r_3. Then R_{ij} is defined by

$$R_{ij}(r_1, r_2, r_3) = \overline{u_{ia}u_{jb}}/(\overline{u_{ia}^2}\,\overline{u_{jb}^2})^{\frac{1}{2}},$$

overbars denoting time averages and u_{ia} the instantaneous value of u_i at station a. The value of y quoted for each set of measurements is that of station a; this can be thought of as a fixed probe (though in practice it may not have been in cases where moving either probe could produce an equivalent change; i.e. $r_2 = \text{const.}$). Positive values of r_1, r_2 and r_3 correspond to station b being at larger x, y and z than station a.

Correlations between u_1 and u_2 are considered in terms of $-R_{12}$ and are shown in the graphs with $-R_{12}$ taken as the positive ordinate. The reason is that the

† The subsequent use in this paper of the term 'large eddies' is not intended to prejudge the outcome of these lines of thought. It is just a convenient shorthand for those 'parts' of the turbulent motion having the largest length-scales—glossing over the issue of the best way of dividing the motion into such 'parts'. Some such division is inherent in all attempts to gain physical understanding of turbulence. An eddy differs from a Fourier component in that the latter has the character of a plane wave of infinite extent whereas the former is considered to be localized; i.e. its extent is of the same order as its length-scale.

sign convention on x and y is such as to make R_{12} at zero separation a negative quantity, whilst it is physically helpful to think in terms of a positive Reynolds stress.

In the discussion of other workers' results, correlations with time separations will be considered. $R_{ij}(r_1, r_2, r_3, t)$ is defined as above except that the signal from station b is taken at a time t later than that from station a.

Other symbols will be defined as they are introduced. Since it is extensively used in the presentation of results, δ_0 is defined here also; it is the distance from the wall at which $U_0 - U = u_\tau$ (U_0 = free stream velocity; U = local mean velocity; u_τ = wall stress velocity).

3. Experimental arrangement

The experiments were carried out in the 20 in. 'low turbulence' wind-tunnel at the Department of Aeronautical Engineering, Indian Institute of Science, Bangalore. A sketch of this tunnel is given in figure 4 of Dhawan & Vasudeva (1959) (the flat plate spanning the centre section shown in this figure was, of course, not there during the present experiments). The boundary layer studied was that on the wooden floor, which was polished before the start of the experiments to ensure smooth wall flow. A trip-wire was stretched across the floor at the end of the contraction to promote regular transition. The test section is slightly divergent to give constant pressure along its length.

All measurements were made with hot-wire anemometers. The traverses carrying these were mounted on a board that formed part of the roof of the tunnel. These were arranged so that one wire could be traversed in the x- and y-directions and a second wire in the z- and y-directions.

The measurements can be regarded as an extension of the work of Grant (1958); hence it seemed a good plan to reproduce fairly closely the conditions of his experiments. The speed outside the boundary layer, U_0, was always within the range 675–710 cm sec^{-1}. The measurements were made around 210 cm (see below) downstream from the trip-wire. This was chosen to be rather more than in Grant's experiments, both to give as thick a boundary layer as possible and to compensate for the difference in kinematic viscosity. These arrangements gave a Reynolds number based on the free-stream velocity and the boundary layer thickness of about $2{\cdot}2 \times 10^4$.

Figures 1 and 2 show the mean velocity profile at $x = 229$ cm, with respectively linear and log-linear co-ordinates. These curves are based on an accumulation of observations during the course of the hot-wire work. The boundary layer extends altogether over about 6·0 cm. δ_0 is the distance from the wall at which $U_0 - U = u_\tau$ and is 3·8 cm (U being the local mean velocity and u_τ being $(\tau/\rho)^{\frac{1}{2}}$, where τ is the wall stress and ρ the density).

u_τ has been determined primarily from the logarithmic part of the profile

$$U/u_\tau = K^{-1}[\ln(yu_\tau/\nu) + A]. \tag{1}$$

Taking $K = 0{\cdot}41$, the straight portion of figure 2 gives u_τ/U_0 as 0·040. However, at Reynolds numbers of the present order, the logarithmic region is less than a

decade in extent and the uncertainty in its slope is rather large. Hence, the determination of u_τ also took into consideration the need to match the regions inside and outside the logarithmic region to 'standard' profiles. In this some compromise was needed. The region close to the wall implied a rather higher value of u_τ, whereas the outer profile would have corresponded more closely to one of the family proposed by Clauser (1956) with a rather lower value of u_τ. This situation arises from the fact that A in (1) is given by figure 2 to be 2·7, a value higher than that usually taken. Another way of saying the same thing is that the

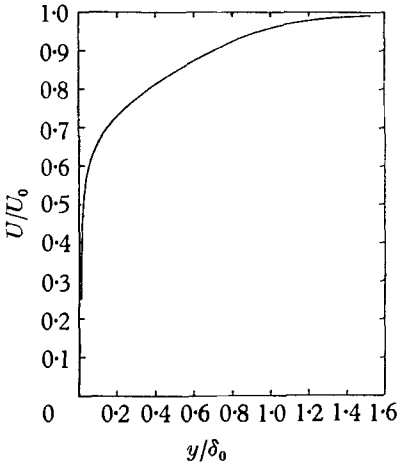

FIGURE 1. Mean velocity distribution.

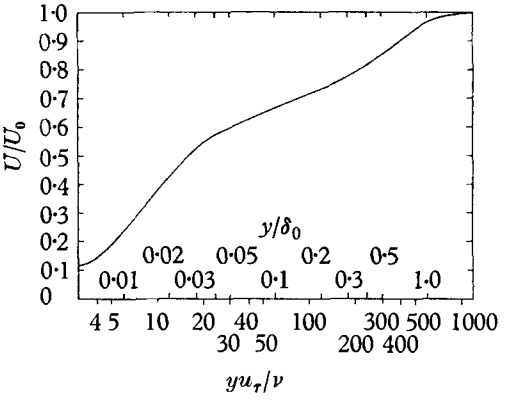

FIGURE 2. Mean velocity distribution.

profile gives $\ln \delta_1/\delta_0$ (where δ_1 is the value of y at which an extrapolation of the logarithmic profile gives $U = U_0$) as 1·15, whereas Townsend (1956, p. 244) quotes 1·37 as the most probable value and Clauser's (1956) profiles correspond to a value of 1·40.

These points need not imply that the boundary layer was not typical; Townsend (1956, p. 243) says that values of A as large as 2·9 have been obtained. They do mean, however, that quantative comparison with Grant's work (regarding values of y/δ_0 and r_i/δ_0) may not be entirely appropriate (Grant's profile gives $\ln \delta_1/\delta_0$ as 1·36).

No detailed measurements of the turbulent intensities were made, but sufficient observations of the signal from a single probe were made to check that variations in intensity across the boundary layer and the relative intensities of different components were typical. A few such measurements were made each time a new hot wire (particularly an X-wire) was introduced, as a check that it was operating satisfactorily. Uncalibrated hot wires could then reasonably be used for correlation measurements.

Because of the need to mount two correctly oriented hot wires in a way that allowed the required traversing without their supports causing obstruction, it was not always convenient to keep x just the same throughout the correlation measurements. x was always between 195 and 230 cm, and for most of the observations between 205 and 215 cm. The mean velocity profile in figures 1 and

2 corresponds to the downstream limit of the x range (because the observations with calibrated hot wires were mostly made before it was found helpful to allow x to vary). Associated with the variations of x will have been variations of δ_0. The data have been evaluated on the assumption that

$$U_0\delta_0/\nu \propto (U_0 x/\nu)^{0\cdot8} \tag{2}$$

(ν is the kinematic viscosity). No theoretical significance is attached to this, but it is typical for the present Reynolds number (Hinze 1959, p. 487) and should be adequate for making a small correction.

Equation (2) could also incorporate corrections to δ_0 for changes in U_0 and ν (the latter varied in the range 0·165–0·18 cm^2 sec^{-1}). However, fluctuations in U_0 during a single run were of the same order as differences between runs, whilst figures 1 and 2 already involve averaging over occasions between which variations in ν occurred. Since the corrections would in any case be small, they have been omitted; i.e. (2) has been used in the form

$$\delta_0 \propto x^{0\cdot8}.$$

The techniques used in the hot-wire anemometry involved nothing novel. Again, Grant's procedures were followed quite closely, some of the electronics being that used by Grant (transferred from Cambridge to Bangalore by the generous permission of Dr A. A. Townsend). The basic features of the system are that it is a constant-current one and that mean-square values of the amplified signal are obtained with a thermo-junction; the correlation of two signals is calculated from the mean-square sum and mean-square difference.

The sensitive portions of some of my wires were rather larger than those used by Grant, but since we are concerned primarily with the behaviour of the correlation functions at large separations, this is of no importance. The same comment applies to errors in the zero of r_i. These were kept small as follows. The whole traverse board could be raised so that the mounted wires were above the tunnel, and their relative location determined quite accurately by eye. The setting for one wire a small distance directly downstream of the other was confirmed by observing when the signal from the former was changed by switching on the heating current through the latter.

The y-zero of a U-wire was determined by making mean velocity measurements in the linear portion of the profile very close to the wall and extrapolating. This was not quite as accurate as expected because of a discrepancy between the slope of the linear portion and u_τ (presumably resulting from extrapolation of the hot-wire calibration). Percentage errors in y/δ_0 might be significant for a few of the measurements very close to the wall, but then the effect of wire length was probably more serious. The value of y for an X-wire was fixed by setting its relative location to a U-wire as described above.

The rather qualitative attitude above to various sources of error is adequate because errors in the correlation measurements themselves are much more serious. Grant's remarks about the accuracy of these apply also to the present work. To these remarks, something must be added about the response of X-wires; since Grant's work, there has been a decline in confidence that X-wires

measure just what is attributed to them. This results partly from observations (Davies, Fisher & Barrett 1963) on the response of a wire to the component of the velocity along its length, and partly from anomalous results appearing in experiments using hot-wire anemometers. The present experiments gave rise to some such anomalous observations, cases in which two measurements which should have been similar according to symmetry considerations differed significantly. These cases contrasted with others in which the agreement was remarkably good. It seems probable that this behaviour was associated with the complexities in the response of a yawed wire, although the apparent absence of any system in the anomalies leaves the connexion vague. My consequent impression is that one can determine the qualitative trends of the correlation functions with reasonable confidence, but that the quantitative results of experiments using X-wires must be treated with more scepticism than has hitherto always been appreciated.

During this work I noticed that the signal from a single probe could be affected —strongly close to the wall—by the approach of a second probe. This is reported separately (Tritton 1967). This is a further source of error, though one does not at present know whether correlations are seriously affected.

4. Results of correlation measurements

Figures 3–21 show the results of the experiments; these figures, rather than any of the text, constitute the main purpose of this paper.

To aid assimilation of the results, continuous curves as well as data points have been put on the graphs, although in a few cases there could be dispute as to the right course of a curve. Occasionally the results are very similar at different stations, and a single curve has been used to summarize two sets of points.

Both the abscissa and the ordinate scales vary from figure to figure, but the fiducial marks are throughout at intervals of 0·2 in r_i/δ_0 and 0·1 in R_{ij}.

The results are presented in a systematic order, unrelated both to the order in which they were obtained and to the reasoning which led to these particular measurements being made. The captions indicate what has been measured and where, but additional comments are needed about some of the results and their presentation.

Figure 5 was intended to be an $R_{11}(r_1, r_2, 0)$ curve with r_1 variable and r_2 constant, and for physical interpretation it can undoubtedly be considered as such. However, subsequent wire-location measurements revealed that r_3/δ_0 actually had the value indicated.

For the reason explained in §2 the measurements of R_{12} are presented and discussed throughout with $-R_{12}$ taken as the positive co-ordinate.

In the representation of some of the $-R_{12}$ results (figures 8–12) by a continuous curve as well as by data points, some value has to be chosen for $-R_{12}$ at zero separation (the normalized Reynolds stress). No systematic survey of this was made during the present experiments, but a number of spot measurements were made during hot-wire testing. One would hesitate to discuss trends across the boundary layer on the basis of these, beyond saying the variations are small for

$0{\cdot}05 < y/\delta_0 < 0{\cdot}8$. The average value of $-R_{12}(0)$ is 0·46. Klebanoff (1955) gives $-R_{12}(0)$ as constant at 0·50 for y/δ_0 less than about 1·2. Townsend's (1951) results imply rather more variation; $-R_{12}(0)$ falls from 0·59 at $y/\delta_0 \simeq 0{\cdot}13$ to 0·48 at $y/\delta_0 \simeq 1{\cdot}0$; it then remains at 0·48 out to $y/\delta_0 \simeq 1{\cdot}3$. The boundary-layer data do not extend to the region very close to the wall; but Laufer's (1954) measurements in pipe flow (as quoted by Rotta (1962)) suggest that $-R_{12}(0)$ does not decrease appreciably until $yu_\tau/\nu < 15$ (though, in Laufer's results, the constant

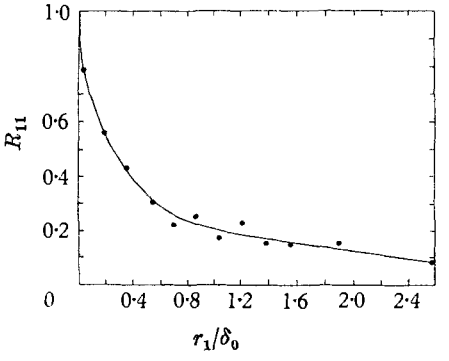

FIGURE 3

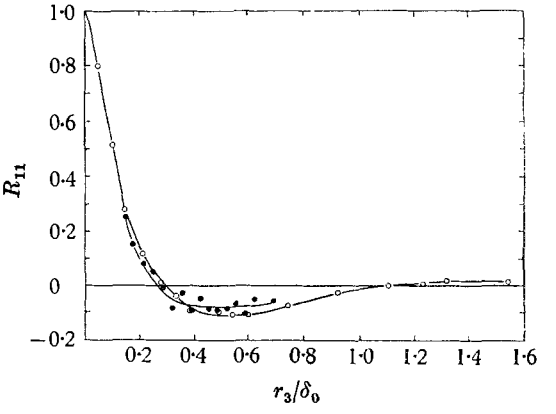

FIGURE 4

FIGURE 3. $R_{11}(r_1, 0, 0)$ at $y/\delta_0 = 0{\cdot}138$.

FIGURE 4. $R_{11}(0, 0, r_3)$ curves at two distances from the wall; ●, $y/\delta_0 = 0{\cdot}138$; ○, $y/\delta_0 = 0{\cdot}305$.

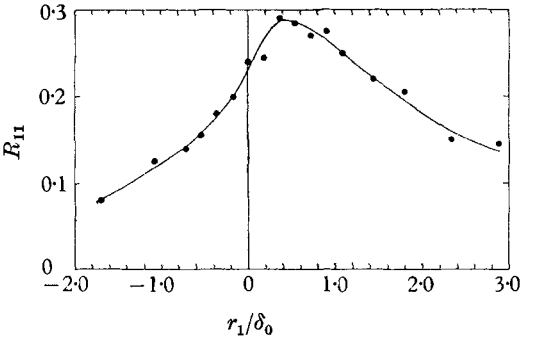

FIGURE 5

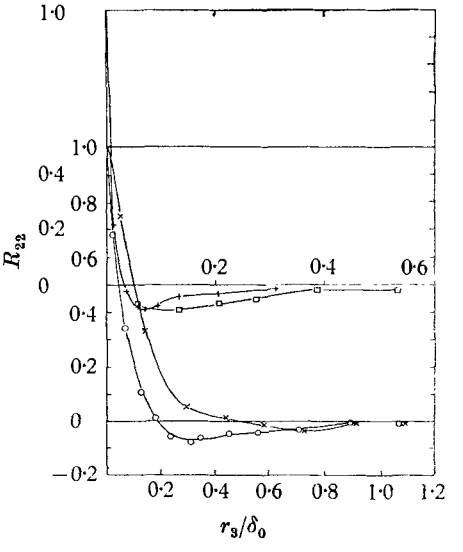

FIGURE 6

FIGURE 5. R_{11} curve with fixed separation normal to the wall and variable separation upstream and downstream; $R_{11}(r_1, r_2/\delta_0 = 0{\cdot}295, r_3/\delta_0 = 0{\cdot}055)$ at $y/\delta_0 = 0{\cdot}159$.

FIGURE 6. R_{22} curves with r_3 separation. Upper abscissa: +, $R_{22}(0, 0, r_3)$; □, $R_{22}(0, r_2/\delta_0 = 0{\cdot}077, r_3)$; both at $y/\delta_0 = 0{\cdot}066$. Lower abscissa: $R_{22}(0, 0, r_3)$ at two distances from the wall; ○, $y/\delta_0 = 0{\cdot}29$; ×, $y/\delta_0 = 0{\cdot}69$. Note different abscissa scales.

value it has outside this is 0·45). In the present experiments $yu_\tau/\nu = 15$ corresponds to $y/\delta_0 = 0{\cdot}025$. The range for which information is needed is $0{\cdot}048 < y/\delta_0 < 1{\cdot}15$, and the curves have all been drawn with $-R_{12}$ taken as 0·50 at zero separation.

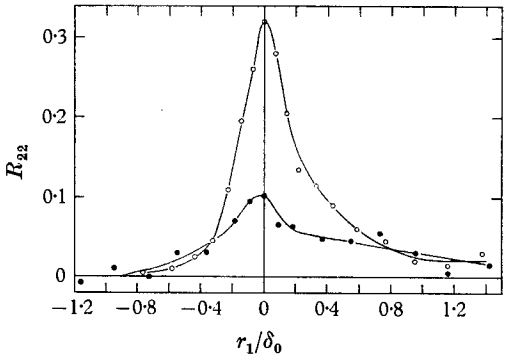

FIGURE 7. R_{22} curves with fixed separation normal to the wall and variable separations upstream and downstream; the two curves are in the same region of the boundary layer but with different r_2; ○, $R_{22}(r_1, r_2/\delta_0 = 0{\cdot}145, 0)$ at $y/\delta_0 = 0{\cdot}21$; ●, $R_{22}(r_1, r_2/\delta_0 = 0{\cdot}29, 0)$ at $y/\delta_0 = 0{\cdot}140$.

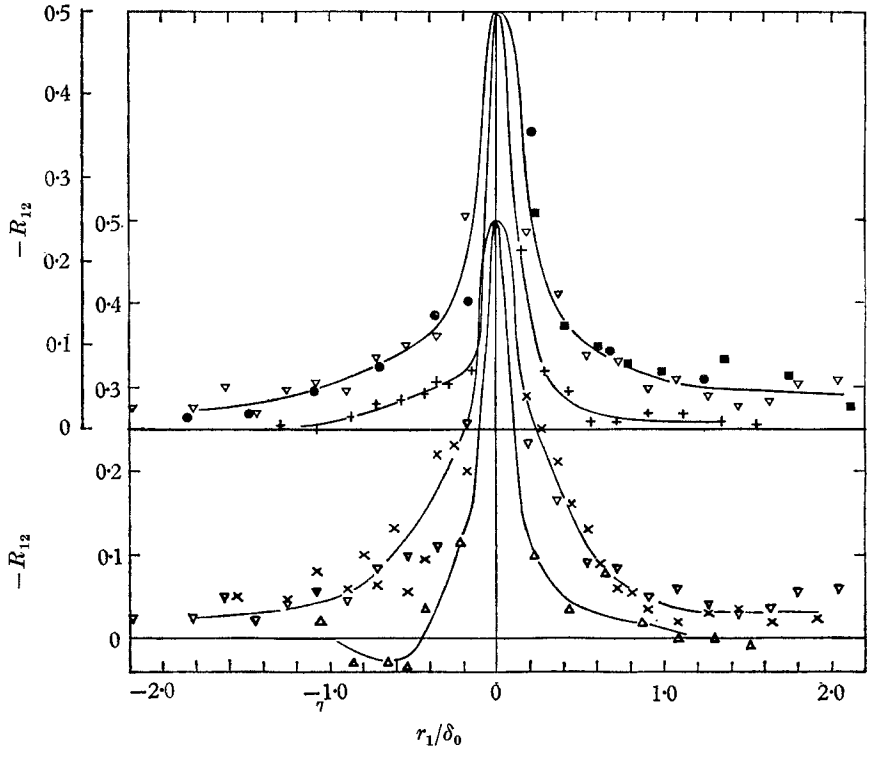

FIGURE 8. $-R_{12}(r_1, 0, 0)$ curves throughout the boundary layer; +, $y/\delta_0 = 0{\cdot}048$; ●, $y/\delta_0 = 0{\cdot}156$; ■, $y/\delta_0 = 0{\cdot}171$ (all on upper abscissa); ▽, $y/\delta_0 = 0{\cdot}51$ (duplicated on the two abscissae); ×, $y/\delta_0 = 0{\cdot}79$; △, $y/\delta_0 = 1{\cdot}15$ (on lower abscissa). Same scale for both abscissae.

Figure 8 shows the behaviour of $-R_{12}(r_1, 0, 0)$ at different distances from the wall. For clarity, some of the curves have a raised abscissa, but, to aid comparison, one set of points ($y/\delta_0 = 0{\cdot}51$) is common to both halves. Results are given for both $y/\delta_0 = 0{\cdot}156$ and $0{\cdot}171$, as the former has only three experimental points for

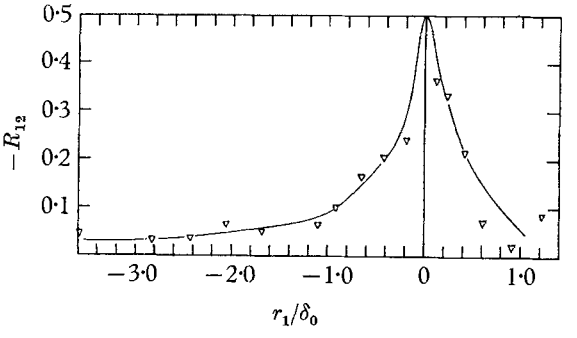

FIGURE 9

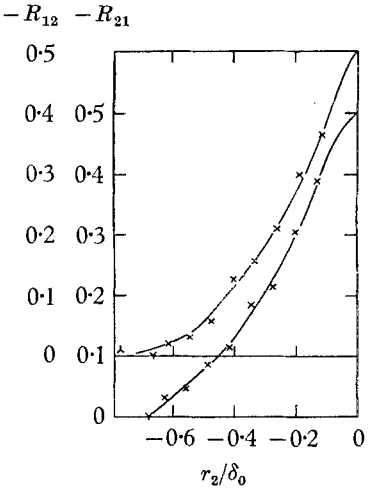

FIGURE 10

FIGURE 9. $-R_{12}(r_1, 0, 0)$ at $y/\delta_0 = 0{\cdot}465$.

FIGURE 10. $-R_{12}$ and $-R_{21}$ curves with negative r_2 separation. Upper abscissa and upper curve: $-R_{12}(0, r_2, 0)$; ×, $y/\delta_0 = 0{\cdot}695$; Y, $y/\delta_0 = 0{\cdot}745$; ⅄, $y/\delta_0 = 0{\cdot}855$. Lower abscissa and lower curve: $-R_{21}(0, r_2, 0)$; ×, $y/\delta_0 = 0{\cdot}705$; Y, $y/\delta_0 = 0{\cdot}755$. (See text.)

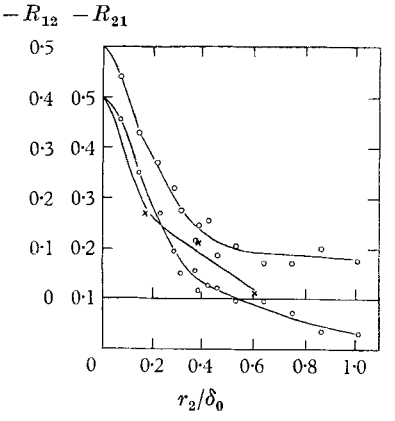

FIGURE 11. $-R_{12}$ and $-R_{21}$ curves with positive r_2 separation. Upper abscissa and uppermost curve: $-R_{12}(0, r_2, 0)$ at $y/\delta_0 = 0{\cdot}29$. Lower abscissa and lower two curves: $-R_{21}(0, r_2, 0)$; ○, $y/\delta_0 = 0{\cdot}29$; ×, $y/\delta_0 = 0{\cdot}685$.

positive r_1, whilst the latter has none for negative r_1. Figure 9 presents measurements of the same type as those in figure 8, but made with the wires mounted so that one could traverse to particularly large negative r_1. The results are interesting as they show $-R_{12}(r_1, 0, 0)$ remaining non-zero to very large separation.

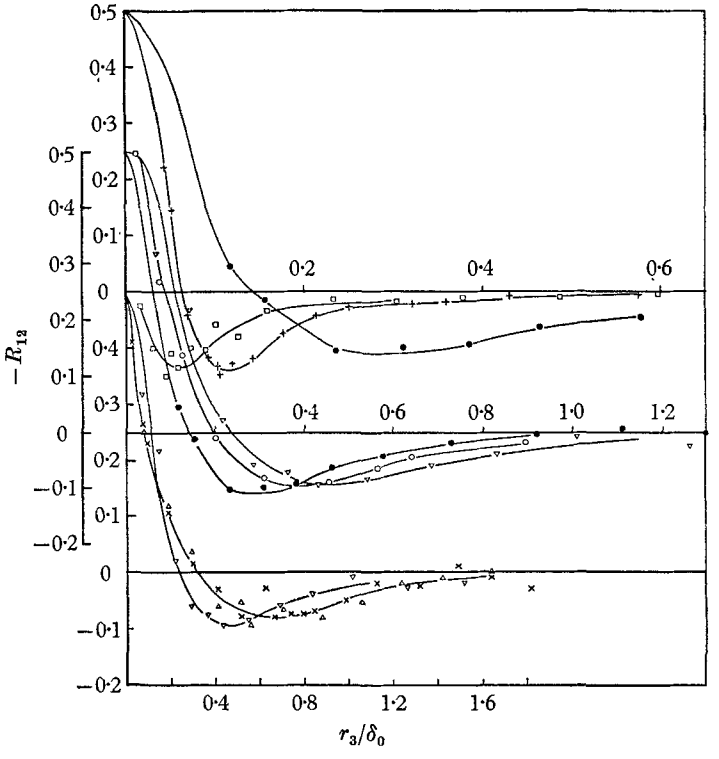

FIGURE 12. $-R_{12}(0, 0, r_3)$ curves throughout the boundary layer; □, $y/\delta_0 = 0{\cdot}017$ (and $r_2/\delta_0 = 0{\cdot}007$, instead of 0); +, $y/\delta_0 = 0{\cdot}049$ (on uppermost abscissa); ●, $y/\delta_0 = 0{\cdot}155$ (duplicated on top and middle abscissae); ○, $y/\delta_0 = 0{\cdot}29$ (on middle abscissa); ▽, $y/\delta_0 = 0{\cdot}51$ (duplicated on middle and bottom abscissae); ×, $y/\delta_0 = 0{\cdot}785$; △, $y/\delta_0 = 1{\cdot}15$ (on bottom abscissa). Note three different abscissa scales.

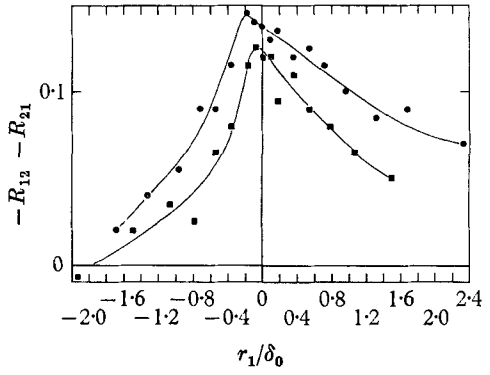

FIGURE 13

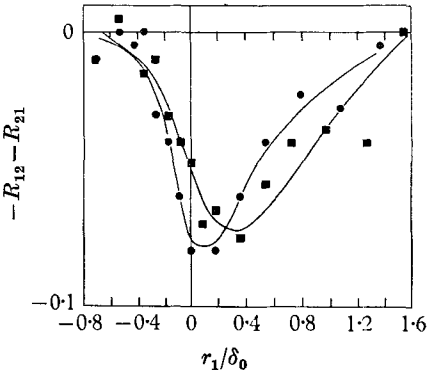

FIGURE 14

FIGURE 13. $-R_{12}$ and $-R_{21}$ curves with fixed separations normal to the wall and variable separations upstream and downstream; ●, $-R_{12}(r_1, r_2/\delta_0 = 0{\cdot}295, r_3/\delta_0 = 0{\cdot}055)$ at $y/\delta_0 = 0{\cdot}158$; ■, $-R_{21}(r_1, r_2/\delta_0 = 0{\cdot}28, r_3/\delta_0 = 0{\cdot}055)$ at $y/\delta_0 = 0{\cdot}163$.

FIGURE 14. $-R_{12}$ and $-R_{21}$ curves with variable separations upstream and downstream and fixed separations in both the other two directions; ●, $-R_{12}(r_1, r_2/\delta_0 = 0{\cdot}22, r_3/\delta_0 = 0{\cdot}325)$ at $y/\delta_0 = 0{\cdot}195$; ■, $-R_{21}(r_1, r_2/\delta_0 = 0{\cdot}21, r_3/\delta_0 = 0{\cdot}325)$ at $y/\delta_0 = 0{\cdot}20$.

Studies of $-R_{12}(0, r_2, 0)$ and $-R_{21}(0, r_2, 0)$ were not so extensive as those of $-R_{12}(r_1, 0, 0)$ (figures 8, 9) and $-R_{12}(0, 0, r_3)$ (figure 12), but an adequate coverage of their behaviour was obtained fairly quickly with the following runs. First, the fixed probe was set near the middle of the boundary layer and the other one

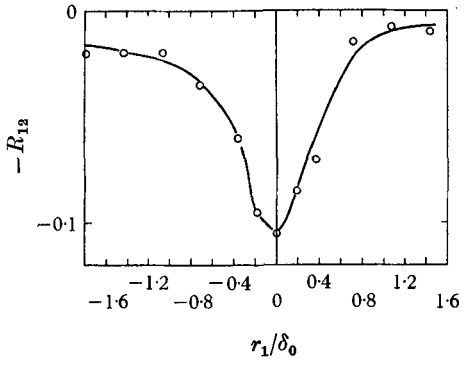

FIGURE 15

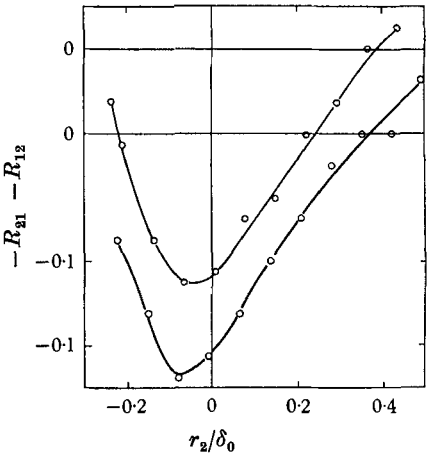

FIGURE 16

FIGURE 15. Variation upstream and downstream of negative region in $-R_{12}$ (non-zero r_3); $-R_{12}(r_1, 0, r_3/\delta_0 = 0{\cdot}325)$ at $y/\delta_0 = 0{\cdot}30$.

FIGURE 16. Variation with separation normal to the wall of negative region in $-R_{12}$ and $-R_{21}$ (non-zero r_3). Upper abscissa and upper curve: $-R_{12}(0, r_2, r_3/\delta_0 = 0{\cdot}325)$ at $y/\delta_0 = 0{\cdot}30$. Lower abscissa and lower curve: $-R_{21}(0, r_2, r_3/\delta_0 = 0{\cdot}325)$ at $y/\delta_0 = 0{\cdot}31$.

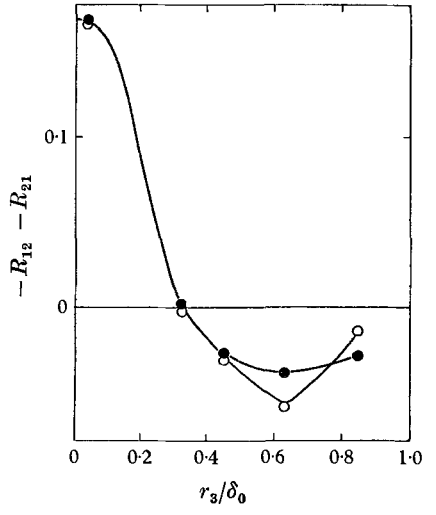

FIGURE 17

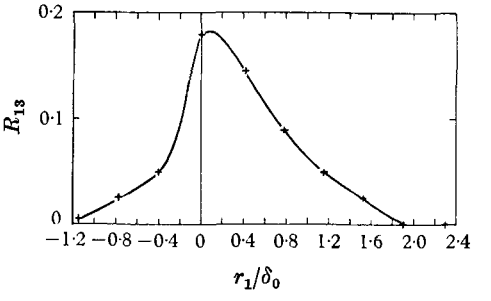

FIGURE 18

FIGURE 17. ●, $-R_{12}(0, r_2/\delta_0 = 0{\cdot}365, r_3)$ at $y/\delta_0 = 0{\cdot}30$; ○, $-R_{21}(0, r_2/\delta_0 = 0{\cdot}35, r_3)$ at $y/\delta_0 = 0{\cdot}31$. (See text.)

FIGURE 18. Variation with separation upstream and downstream of R_{13} close to the wall (non-zero r_3); $R_{13}(r_1, 0, r_3/\delta_0 = 0{\cdot}185)$ at $y/\delta_0 = 0{\cdot}029$.

traversed towards the wall; when it could go no closer, the range of r_2 was extended a little by taking the previously fixed probe to slightly larger y (figure 10). In another pair of runs the fixed probe was nearer to the wall and the moving one traversed towards the outer edge of the boundary layer (figure 11). Finally, a few readings of $-R_{21}$ only were taken with the fixed wire in the middle of the boundary layer and the moving one going outwards.

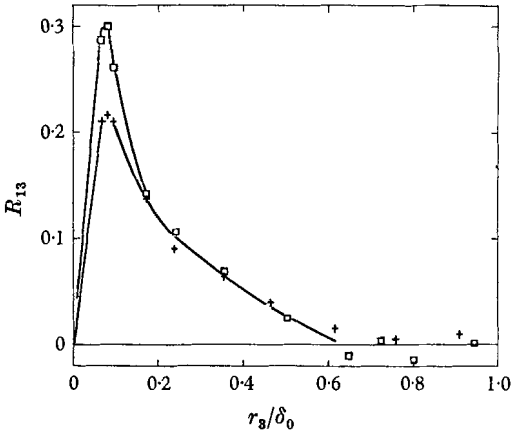

FIGURE 19

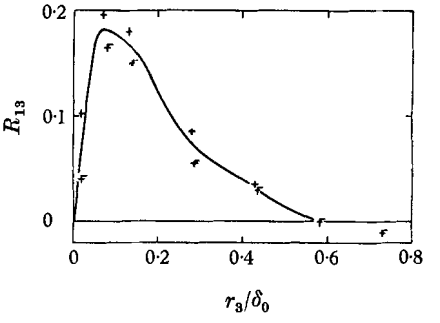

FIGURE 20

FIGURE 19. Variation of R_{13} with r_3 close to the wall; +, $R_{13}(0, r_2/\delta_0 = 0{\cdot}007, r_3)$ at $y/\delta_0 = 0{\cdot}032$; □, $R_{13}(0, r_2/\delta_0 = -0{\cdot}015, r_3)$ at $y/\delta_0 = 0{\cdot}054$.

FIGURE 20. $R_{13}(r_1/\delta_0 = 0{\cdot}395, r_2/\delta_0 = 0{\cdot}007, r_3)$ at $y/\delta_0 = 0{\cdot}032$; the flagged points correspond to measurements with both r_3 and R_{13} having opposite sign from the rest.

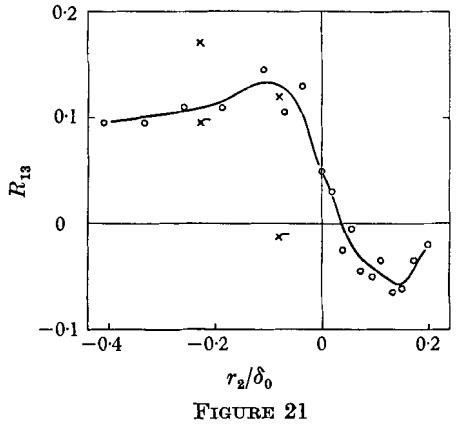

FIGURE 21

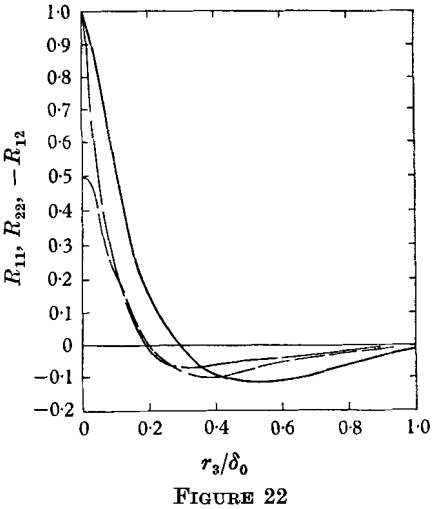

FIGURE 22

FIGURE 21. ○, $R_{13}(0, r_2, r_3/\delta_0 = 0{\cdot}15)$ at $y/\delta_0 = 0{\cdot}445$; +, $R_{13}(0, r_2, r_3/\delta_0 = 0{\cdot}21)$ at $y/\delta_0 = 0{\cdot}445$; the flagged points correspond to measurements with both r_3 and R_{13} having opposite sign from the rest. (See text.)

FIGURE 22. Comparison of R_{11}, R_{22}, and $-R_{12}$ curves with r_3 separation in one part of the boundary layer. ——, $R_{11}(0, 0, r_3)$ at $y/\delta_0 = 0{\cdot}305$; – – – –, $R_{22}(0, 0, r_3)$ at $y/\delta_0 = 0{\cdot}29$; — — —, $-R_{12}(0, 0, r_3)$ at $y/\delta_0 = 0{\cdot}29$.

Figure 12 shows the behaviour of $-R_{12}(0, 0, r_3)$ at various distances from the wall. (r_2 was not quite zero in the survey closest to the wall, because of the size of an x-wire probe). As in figure 8, vertical separations have been introduced for clarity, this time into three groups. Note the changes in abscissa scale between groups. So that the trend with y/δ_0 can readily be seen despite these, one set of points ($y/\delta_0 = 0{\cdot}153$) is common to the two top groups and another set ($y/\delta_0 = 0{\cdot}51$) to the two bottom groups.

The comment above about figure 5 applies also to figure 13. The curves in this may be thought of as $-R_{12}(r_1, r_2, 0)$ and $-R_{21}(r_1, r_2, 0)$ (r_1 variable, r_2 fixed).

Figures 18–21 present measurements of R_{13}. These experiments had an unsatisfactory feature. A check that the hot-wire anemometers are behaving as supposed may be made by changing the sign of r_3; R_{13} for instance should be antisymmetric with respect to r_3. Departures from the theoretical behaviour are most likely to be due to the uncertainties of X-wire operation considered in §3. The R_{13} measurements contained serious discrepancies of this sort, although they also contained measurements that seemed remarkably consistent. These latter are shown in figure 20 (flagged points correspond to measurements with the sign of both r_3 and R_{13} changed compared with unflagged points). These measurements were made at an early stage of the sequence of experiments reported by figures 18–21 and encouraged me to continue. Towards the end of the work the measurements of figure 21 were made (the stations at which measurements with reversed r_3 were made were governed partly by the need to avoid collision of the traverses) and raised doubts about just what was being measured. No straightforward cause of the discrepancy could be found. Obviously further measurements with different wires should have been made. Unfortunately, the experimental programme had to be ended before I had done this. The matter did not seem specially urgent, as, despite the discrepancies, the qualitative features of the R_{13} pattern that are of physical interest (see §6) can be inferred, without great hesitation, from the measurements; although the quantitative details are clearly in considerable doubt.

5. Vibrating ribbon experiment

The foregoing experiments were started in conjunction with some experiments on the effect of a vibrating ribbon in the turbulent boundary layer. These latter were largely unsuccessful, but a very brief account of them may be useful.

The idea was to test the conjecture that the large eddies (or some of them) originate as an instability of the viscous sublayer, by performing experiments in a turbulent boundary layer similar to those that promote instabilities in a laminar boundary layer. The arrangement was similar to that used by a number of workers, starting with Schubauer & Skramstad (1947), in laminar boundary layers, except for a few changes necessary to permit larger amplitudes. The ribbon extended outside the tunnel through slots in the wall, so that it could be in the strongest part of the field of U-shaped magnets and so that the amplitude could be observed. The tension in the ribbon was controlled so that the vibration was always at resonance. The ribbon was about 0·005 cm thick and 0·1 cm wide. No significant effect of its vibrations on the intensity or on $R_{11}(r_1, 0, 0)$ at large

r_1 was observed with the frequency varied through the range 5–800 c/s. The amplitude was rather variable, but typically such as to give a velocity amplitude of 50 cm sec^{-1}. Several geometrical arrangements were tried. However, one cannot put any great confidence in the negative result in view of unsatisfactory features. It was difficult to prevent the ribbon from undergoing flutter. When this was achieved, it was still difficult to keep the ribbon untwisted, so that it did not significantly obstruct the flow and produce intensity changes even when it was not vibrating.

Thus, if anything, these experiments point against the view that the large eddies arise from sublayer instability. One would not wish to hold to this inference in the face of contrary evidence, but it is perhaps worth considering in conjunction with the evidence in the correlation measurements (see §9) against the view that the outgoing parts of the large eddies are more coherent than the ingoing parts.

6. Large eddies and the Reynolds stress

The contribution of the large eddies to the Reynolds stress is a matter of considerable importance for the calculation of mean flow development in complicated practical configurations. Yet, when one tries to extract information about this from the experimental data, one cannot be sure of the sign of the effect let alone its magnitude. Some lines of reasoning raise the interesting possibility that the large eddies might make a negative (i.e. of opposite sign to the total) contribution to the Reynolds stress in parts of a boundary layer; others do not confirm this. The following discussion of this point is also germane to Townsend's (1957, 1961) suggestion that the turbulence in the inner part of a layer can be considered as a 'universal motion' plus an 'irrelevant motion', the latter not contributing to the Reynolds stress.

The large eddies probably travel downstream at a speed characteristic of the boundary layer as a whole rather than at the local mean velocity (see, for example, Sternberg 1962). Close to the wall, therefore, their speed is likely to exceed the mean speed. Also, it has been suggested that a characteristic feature of the large eddies is a coherent jet-like motion away from the wall, continuity being satisfied by a diffuse weak motion towards the wall. This feature is part of Grant's, Townsend's and Lilley's models, and it is Kline & Runstadler's interpretation of their dye observations. The combination of motion away from the wall and motion downstream faster than the local mean velocity would give a negative contribution to the Reynolds stress. This in turn would imply a local transfer of energy from the eddies to the mean flow, but this is possible provided that the effect is local and the transfer is in the reverse direction in other parts of the boundary layer.

Some support, albeit far from conclusive, for this inference is to be found in the data of Favre *et al.* (1957, 1958). An oversimplified expression of this is that the '*maximum maximorum*' of Favre *et al.* moves outwards and also downstream faster than the mean velocity. Since Grant (1958, §4.4) suggested that the outward movement corresponded to the outward jets of his large eddy model, it has been found that the *maximum maximorum* can move outwards when one traces it upstream as well as downstream (i.e. the right-hand half of figure 7 of Favre *et*

al. (1958) has been filled in). The interpretation might, however, be maintained when there is asymmetry between the upstream and downstream curves. Then, referring to figures 7–9 of Favre *et al.* (1958), the evidence for the outward movement is strong in the outer part of the boundary layer, weak in the inner part. The evidence for the fast downstream motion emerges, tentatively, from an examination of the time delays associated with the *maximum maximorum*. The details will not be given here, but the argument can be summarized by reference to figure 5 of Favre *et al.* (1958); where this shows a difference between the measured and 'computed' optimum time delays the former is the smaller. Refinements to this comparison to make it more relevant to the present considerations do not alter the regions in which the difference may be significant. Thus, there is evidence for a fast downstream motion in the inner part of the boundary layer, not in the outer. No evidence for a downstream motion slower than the local mean speed in the outer part emerges in this way. On the other hand, Sternberg (1962), examining a different part of Favre *et al.*'s data, finds both fast advection close to the wall and slow far from it.

Hence, one needs to ask whether, as one goes away from the wall, the evidence for a predominantly outward motion becomes significant before the evidence for a fast downstream motion ceases to be significant. This is very difficult to decide, but the possibility seemed strong enough that the above considerations were one of the main motives for my own experiments.

There is another way in which Favre *et al.*'s data seemed to point to a negative large eddy contribution to the Reynolds stress, although the implied mechanism does not correspond to the physical model discussed above. The data imply that $R_{11}(0, r_2, 0, t)$ maximized with respect to t is greater than $R_{11}(r_1, r_2, 0, 0)$ with r_1 chosen so that the maximum of $R_{11}(r_1, r_2, 0, t)$ is at $t = 0$. (This comes from a consideration of figure 7 of Favre *et al.* (1958) in conjunction with information on the optimum time delays.) Since the time delay for the maximization of the former correlation is negative (i.e. the signal is taken earlier from the outer probe), the fact that the former correlation is greater than the latter is difficult to interpret without postulating a marked inward motion that is moving downstream slowly. Such a motion would contribute negatively to the Reynolds stress. The only objection to this argument that I can see is that it is based on rather few experimental points.

Experiments giving further information on this matter were clearly needed, but, as often, there is no experiment that gives a definite direct answer to the question; one has to make those that seem likely to give an indirect answer. This was the motivation for many of the observations on $-R_{12}$ and R_{13} reported in §4.† The measurements of $-R_{12}(r_1, 0, 0)$ and $-R_{12}(0, 0, r_3)$ at rather many

† At first sight, measurements of the spectrum of the Reynolds stress might seem most appropriate, and information on this is available (Klebanoff 1955). However, the use of this is restricted, because one can measure only the one-dimensional spectrum function and because the low wave-number end of such spectra depends on eddies of all sizes rather than just the large eddies (Townsend 1956, pp. 17–18). It therefore seemed more useful to make correlation measurements; those of $-R_{12}$ with separation in the r_1-direction give substantially the same information as the spectrum measurements in a more appropriate form, whilst those with separation in other directions give much additional information.

values of y derive from the fact that any exceptionable behaviour was likely to be confined to a fairly small part of the boundary layer.

In retrospect, the measurements of $-R_{12}$ and R_{13} contain a number of interesting features without fully answering the question originally asked of them. It is convenient to discuss all these features together and then to turn to the implications of some of them about the large eddy contribution to the Reynolds stress.

One noteworthy feature is a tendency for $-R_{12}(y, r_1, r_2, r_3)$ and $-R_{21}(y, r_1, r_2, r_3)$ to be nearly the same even when there is no symmetry requirement for them to be so; i.e. interchanging the positions of measurement of u_1 and u_2 has little effect on the correlation (compare the left-hand side of figure 8 with the right-hand side, and the different curves in figures 10, 11, 13, 14 and 16). There are differences to be detected; for example, figures 8 and 9 suggest a tendency for the correlation to fall off from its maximum at $r_1 = 0$ more rapidly when r_1 becomes negative than when it becomes positive. However, these differences are small and may no often be significant; considering again the example just mentioned, this may be only the result of one wire being in the wake of the other.

Another point of interest is the large values of $\pm r_1$ to which $-R_{12}$ remains non-zero. This is to be found at all values of y/δ_0 except the smallest and the largest (figure 8) and is illustrated particularly by figure 9 (note the compressed abscissa scales in these figures). The corresponding observation for R_{11} has been an important factor in the development of ideas about the large eddies (by, for instance, Townsend (1957)). We now need to comprehend how the eddies can be extended in the direction of flow in such a way as to produce this effect in R_{11}, $-R_{12}$ and $-R_{21}$, but not in R_{22}. The point may be illustrated by considering the behaviour when y/δ_0 is a little greater than 0·1. R_{11} falls to 0·2 at r_1/δ_0 of about 1·0 and to 0·1 at about 2·3 ($y/\delta_0 = 0{\cdot}14$; figure 2); $-R_{12}$ and $-R_{21}$ both fall from their maximum of 0·5 to 0·1 at r_1/δ_0 of about 0·6 and to 0·05 at about 1·1 ($y/\delta_0 = 0{\cdot}155$; figure 8); whilst R_{22} becomes zero at r_1/δ_0 about 0·4 and goes only very slightly negative beyond this ($y/\delta_0 = 0{\cdot}13$; Grant (1958)).

The most striking point in the behaviour of $-R_{12}$ is the change of sign with r_3 separation (figure 12). This is shown right through the boundary layer, and minimum values of $-R_{12}$ vary from about $-0{\cdot}13$ close to the wall to $-0{\cdot}08$ in the outer part of the layer. These negative values are as large as or larger than those exhibited by R_{ii} correlations, despite the fact that R_{ii} at zero separation is unity whilst $-R_{12}$ is only about 0·5. It seemed valuable to ascertain as much as possible about the magnitude and extent of the negative $-R_{12}$ region; this was the purpose of the work contained in figures 14–17.†

The interpretation of the behaviour of $-R_{12}$ obviously has to be made with the corresponding behaviour of R_{11} and R_{22} borne in mind. Figure 22 collects together (from figures 4, 6 and 12), curves for $R_{11}(0, 0, r_3)$, $R_{22}(0, 0, r_3)$ and

† The purpose of figure 17 may not be obvious. Figure 16 suggests that $-R_{12}(0, r_2, r_3)$ and $-R_{21}(0, r_2, r_3)$ become positive when r_2 is large enough. This might indicate a limit to the negative region. On the other hand it might be the result of increased length-scale (due to the average distance of the two probes from the wall being larger) shifting the negative region to larger r_3. The observations shown in figure 17 were made to decide between these two possibilities—in favour of the latter.

$-R_{12}(0, 0, r_3)$ at similar values of y.† The feature of R_{22} and $-R_{12}$ changing sign at just about the same value of r_3/δ_0 is largely a coincidental result of the particular value of y/δ_0 for which observations of all of R_{11}, R_{22} and $-R_{12}$ have been obtained. Close to the wall R_{22} becomes negative for smaller values of r_3 than $-R_{12}$ (compare figure 6 and the top section of figure 12). More interesting perhaps is the reverse behaviour at large y/δ_0. The bottom section of figure 12 shows that $-R_{12}$ changes sign at r_3/δ_0 of about 0·24 and 0·32 for y/δ_0 equal to respectively 0·51 and 0·785; figure 6 shows R_{22} at $y/\delta_0 = 0{\cdot}685$ remaining positive for r_3/δ_0 up to about 0·49, and then it goes only weakly negative.‡ Interpolation in figure 12 suggests that $-R_{12}$ may be approaching its minimum value before R_{22} changes sign. Moreover, it is unlikely that R_{11} changes sign at separations as small as those for $-R_{12}$. The present results do not contain information on this point, but Grant's results at $y/\delta_0 = 0{\cdot}52$ show $R_{11}(0, 0, r_3)$ changing sign at r_3/δ_0 of about 0·36. It is almost certain that in the outer part of the boundary layer there are lateral separations for which $-R_{12}$ is negative but R_{11} and R_{22} are both positive.

The R_{13} measurements reported by figures 18–21 can be viewed in a comparatively straightforward manner. In isotropic turbulence, such correlations would always be zero for $r_1 = 0$. The departures from this shown by figures 19 and 21 must be associated with departures from isotropy and can in fact be related to the Reynolds stress. The partial similarity to isotropic turbulence that is always imposed by the continuity equation is likely to produce a correlation between u_2 and u_3 when both r_2 and r_3 are non-zero. The association between u_1 and u_2 involved in the Reynolds stress then leads one to expect $R_{13}(0, r_2, r_3)$ to behave similarly to the actual behaviour shown by figure 21. The sign of R_{13} indicated in this way is in agreement with the experimental results if we suppose that the large eddies produce a Reynolds stress of the same sign as the total stress.

For low values of y/δ_0 the argument is modified by the further departures from isotropy that will be imposed by the proximity of the wall. Any velocity fluctuation towards or away from the wall is likely to be associated with a flow pattern in the turbulence resembling a stagnation point flow. A correlation between u_2 and u_3 with separation in the r_3 direction may be expected even if $r_2 = 0$. The association between u_1 and u_2 involved in the Reynolds stress then suggests that $R_{13}(0, 0, r_3)$ will be non-zero. Figure 19 shows that this is indeed the case. The sign is again such that the argument applies provided that we consider a Reynolds stress of the usual sign. The two curves in figure 19 show that $R_{13}(0, r_2, r_3)$ with r_3 variable has a larger maximum for a negative r_2 than for a (smaller) positive one. This is in accord with the above interpretation, considering the effect of continuity as before.

Figure 18 shows the effect of varying r_1. For isotropic turbulence, $R_{13}(r_1, 0, r_3)$ would of course be positive for positive r_1 and negative for negative r_1 (since r_3 is

† The value of y for the R_{11} curve is a little different than for the other two. A few measurements of $R_{11}(0, 0, r_3)$ at $y/\delta_0 = 0{\cdot}290$ were made and showed no significant difference from those at 0·305 (with regard particularly to the zero and the minimum).

‡ This result is only a confirmation of one of Grant's (1958). Confirmation seemed desirable, however, as the present results and Grant's are not in complete agreement about the behaviour of $R_{22}(0, 0, r_3)$ (see §8).

taken positive). We see that this effect is superimposed on the one considered above, so that R_{13} is positive throughout but asymmetrical.

What can now be said about the sign of the large eddy contribution to the Reynolds stress? The matter just discussed—the interpretation of non-zero R_{13}, when $r_1 = 0$—seems the most conclusively relevant. It provides clear evidence against the idea of a negative contribution. This is to some extent true for all parts of the boundary layer, but is most definite for the region close to the wall. Further implications of this conclusion will be considered briefly in § 9.

The $-R_{12}$ measurements are not so directly revealing. However, the fact discussed above, that at large y, $-R_{12}$ changes sign as r_3 is increased sooner than either R_{11} or R_{22}, is curious. We might also note that, at still larger y, figure 8 shows (perhaps not very conclusively) $-R_{12}(r_1, 0, 0)$ going slightly negative for negative r_1 (though not for positive). But for the fact that this is the part of the boundary layer where there is least other reason to expect a negative large eddy contribution to the Reynolds stress, these points might be taken to suggest that one occurs. Further clarification of this unsatisfactory situation seems likely to come about not through direct interpretation of the data but rather through a new model of the large eddies consistent with the data.

7. Upstream–downstream asymmetry

A result of Favre *et al.*'s (1957) work to which some attention has been given is that $R_{11}(0, r_2, 0, t)$ has its maximum value (for fixed r_2) at non-zero t. Measurements by Bowden (1962) and Bowden & Howe (1963) in tidal channels suggest that if one considers instead $R_{22}(0, r_2, 0, t)$ this skewness is no longer found; the maximum is at zero t. This is inconsistent with the usual interpretation of the asymmetry—that the large eddies are orientated along a line at about 45° to the flow direction—and one has to reconsider the significance of these results. Hence, it seemed desirable to check the oceanographic observations in the better-defined conditions of the laboratory.

There was no equipment available for introducing time delays into the correlation measurements. Hence I adopted the more-or-less equivalent procedure of measuring $R_{22}(r_1, r_2, 0)$ with r_2 fixed and r_1 varied. There are a few measurements of this type in Grant's work, but it seemed desirable to extend them. So that a direct comparison could be made, I also made a few observations of $R_{11}(r_1, r_2, 0)$. Since much of the project was concerned with the behaviour of $-R_{12}$ and since it might be revealing about the significance of the asymmetry, I included further some measurements of $-R_{12}(r_1, r_2, 0)$, $-R_{21}(r_1, r_2, 0)$, $-R_{12}(r_1, r_2, r_3)$ and $-R_{21}(r_1, r_2, r_3)$. These last two were surveyed with r_3 fixed so that $-R_{12}$ and $-R_{21}$ were significantly negative in the hope of discovering more about the striking negative region discussed in § 6.

The results are shown in figures 5, 7, 13 and 14 and reveal an interesting situation.

The result that $R_{22}(r_1, r_2, 0)$ with r_2 fixed has its maximum at $r_1 = 0$ is confirmed (figure 7). The curves are nevertheless asymmetric, the correlation tending to zero much more slowly on the positive r_1 side than on the negative. In this

respect the behaviour is similar to that of R_{11}. Figure 7 accords with and supplements Grant's (1958) figure 23, which presents similar observations for larger y/δ_0. The figures differ in that Grant's shows R_{22} becoming negative—strongly for positive† r_1 and less markedly for negative. The difference is consistent with the observation (Grant 1958) that $R_{22}(r_1, 0, 0)$ goes negative in the outer part of the boundary layer but not in the inner. Both lots of results may be summarized by saying that, for positive r_2, the tail of $R_{22}(r_1, r_2, 0)$ is longer on the positive r_1 side, be it a positive or a negative tail.

Similar considerations apply to $-R_{12}$. Figure 13 shows that $-R_{12}(r_1, r_2, 0)$ and $-R_{21}(r_1, r_2, 0)$ tend to zero much more slowly on the positive r_1 side. As with R_{22} (but not with R_{11}), this contrasts with the behaviour for small r_1/δ_0; the maximum

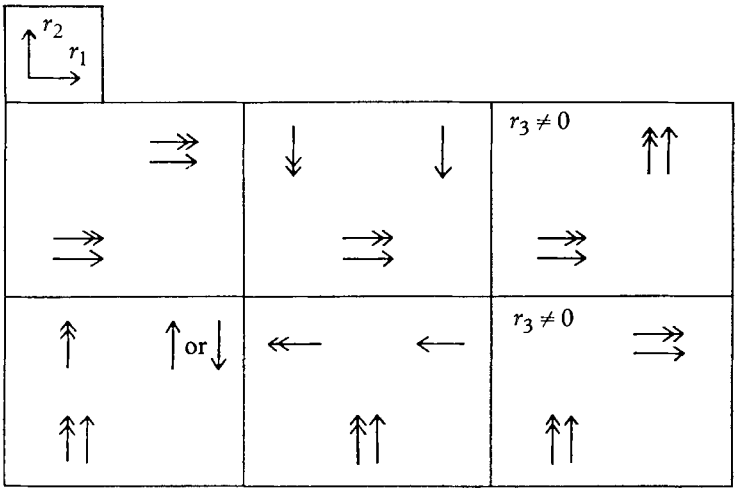

FIGURE 23. Schematic representation of the correlations with r_1 variable and r_2 fixed but non-zero. Single-headed arrows refer to the behaviour at large $\pm r_1$. Double-headed arrows refer to the position of maximum correlation. (See text.)

is not displaced in the same way. Indeed, there is evidence (though it might be argued that the differences in the correlation coefficient on which this is based are not large enough to be significant) that the maxima in figure 13 occur at slightly negative r_1/δ_0. The word 'slightly' is used here in relation to the overall r_1 scale of the graphs; it needs to be remembered that this is compressed and that the displacement from zero is not so small when compared with r_2/δ_0. This position of the maxima can be related to the continuity equation; in isotropic turbulence $-R_{12}(r_1, r_2, 0)$ and $-R_{21}(r_1, r_2, 0)$ would both be positive for negative r_1 and negative for positive (taking r_2 positive).

Figures 14 show similar observations with an r_3 displacement introduced to make $-R_{12}$ and $-R_{21}$ negative. These can be fitted into the same interpretation. The effect of continuity would now be to displace the peak (a minimum this time) to the positive r_1 side. This is in the same direction as the asymmetry of the tails

† Changing the sign of r_1 to allow for the fact that Grant had r_2 negative whereas we are considering its positive [$R_{22}(y; r_1, r_2, 0) \equiv R_{22}(y + r_2; -r_1, -r_2, 0)$].

that runs throughout the observations. It is thus accordant that these curves should be more or less symmetrical about displaced peaks.

A convenient visual summary of the situation is given in figure 23. The directions of the arrows indicate the velocity fluctuation components under consideration and their relative locations indicate the signs of r_1 and r_2 for which the correlation between these tends to be strong. The single-headed arrows are based on the asymmetry of the tails of the correlation curves; the double-headed arrows are based on the peaks of the correlation curves. The figure demonstrates clearly the tendency for the former to have the same relative location throughout (presumably a consequence of the shear of the mean flow), whilst the latter have the relative location suggested by continuity.

8. Boundary layer and channel flow

It is of some theoretical significance to compare these two flows, particularly for the regions close to the wall. The fact that some correlation length-scales can much exceed the distance from the wall has complicated the concept of wall similarity and suggested that some features of the turbulence may be influenced by the outer region; in the phraseology of Townsend (1957, 1961), the scale of the 'irrelevant motion' may be imposed on the wall layer by the outer layer. Since the turbulence in the outer regions of a boundary layer has a different structure from that of channel flow, it is interesting to look for any consequent differences in the wall layers.

A comparison of Grant's (1958) boundary-layer data and Comte-Bellot's (1961*b*) channel flow data suggested that there might be differences—in two ways, one implying a difference in structure, the other a difference in scale. It was, however, inconclusive. Some of the present results were obtained to allow closer comparisons and they suggest that the differences are not significant.

The comparisons will be made with lengths in the boundary layer non-dimensionalized with δ_0 as usual and those in the channel with its half-width, D. There is no reason to suppose that these give strictly comparable quantities, but they should be satisfactory for the present purpose so long as a scale typifying the flow as a whole is appropriate. It might be argued that, since we are concerned with the wall layer, the length-scale ν/u_τ should be taken. This would change the comparisons radically because of the difference in Reynolds number of the flows being compared (Comte-Bellot worked with $u_\tau D/\nu$ equal to about 5000,† whereas $u_\tau \delta_0/\nu$ was about 700 in Grant's experiments and about 600 in mine). One supposes that similar changes follow a change of Reynolds number in a single type of flow, and thus that this is a separate issue from the comparison of different types. We are saying only that one of the available methods of scaling now shows no significant differences between the two flows.

The possibility of a difference in structure was raised by the fact that Comte-Bellot's results show $R_{22}(0, 0, r_3)$ having a negative region (for her lowest value of y/D, 0·11) whereas Grant's do not ($y/\delta_0 = 0{\cdot}059$). Figure 6 shows that my measurements gave a negative region; indeed, at $y/\delta_0 = 0{\cdot}066$ and 0·29, it is sur-

† The additional information about the channel and the flow in it needed for the comparisons has been taken from two of Comte-Bellot's earlier papers (1959, 1961*a*).

prisingly marked. The upper section of figure 6 is in disagreement with Grant's results, the difference in y/δ_0 being certainly insufficient to account for this. The reason is not known.

The possibility of a difference in scale arose from considerations of the extent of $R_{11}(r_1, 0, 0)$. This is the correlation that shows most strongly the failure to obey the principle that the length-scale close to the wall is given by the distance from the wall. For channel flow, Comte-Bellot's results at $y/D = 0{\cdot}11$ show R_{11} dropping to 0·2 at r_1/D of about 1·4 and to 0·1 at about 2·1. In Grant's boundary layer results, the corresponding values of r_1/δ_0 were about 0·5 and 0·8. These were at $y/\delta_0 = 0{\cdot}034$, but the similarity of this behaviour to that at much larger y/δ_0 made it tempting to suppose that a comparison was valid. Figure 3 of the present paper shows that this is not the case; at $y/\delta_0 = 0{\cdot}14$, R_{11} drops to 0·2 at about $r_1/\delta_0 = 1{\cdot}0$ and to 0·1 at about 2·3.

9. Closing remarks

Even before my experiments there was a large body of data that had not been incorporated into any model of the large eddies. An obvious aim now is to formulate ones consistent with all the information existing. As stated in § 1, I have not had much success in this. It may be useful, however, to note that the principal features of the present results that probably ought to be taken into account in any such formulation.

The discussion in § 6 of the $-R_{12}$ results contains a number of points with implications wider than the matter of that section. The strong tendency for $-R_{12}$ and $-R_{21}$ to be nearly the same is one such point; some differences were noted, but a new large eddy model would probably need to attend to the similarities rather than the differences.

A second point is the behaviour at large r_1. This has already been briefly discussed in § 6; here we just need to note again that it is curious—and surely relevant to the large eddy structure—that R_{11}, $-R_{12}$ and $-R_{21}$ all remain significantly non-zero when R_{22} does not.

Thirdly, there is the striking change of sign in $-R_{12}(0, 0, r_3)$. Although this is one of the ways in which the new observations are inconsistent with existing models of boundary-layer structure, such a behaviour would seem to require a high degree of ordering of the large eddies. It could hardly come about unless the eddies have a characteristic structure and orientation. This is perhaps the main reason, despite lack of success so far, for continuing to look for a simple structural model of the eddies of the types proposed by Townsend and Grant (see § 1) rather than turning to a different type of description.

The negative region of $-R_{12}(0, 0, r_3)$ prompts a further thought. It is a strong feature throughout the boundary layer, and it would be most satisfactory if a single interpretation of it for all y could be formulated. More generally, looking at all the information now available, one might say that the similarities between the inner and outer parts of the boundary layer are more marked than the differences. Perhaps the practice that has been adopted in the past of giving quite separate descriptions of the large eddies for the two regions is no longer appropriate.

It was pointed out in §6 that the combination of a coherent motion away from the wall and a fast downstream motion would result in a negative contribution to the Reynolds stress in the region close to the wall. But it is in this region that the evidence against such a negative contribution is strongest. Assuming only that velocity fluctuations towards and away from the wall produce flow patterns of a stagnation point flow type, a negative contribution to the Reynolds stress would involve a change of sign of $R_{13}(0, 0, r_3)$ at large separations. The results show no such change. That the large eddies in the wall region do travel downstream faster than the local mean velocity seems satisfactorily established by Sternberg (1962). This suggests that the feature, common to most existing models, of a coherent eruption from the viscous sublayer with a more diffuse return flow should be abandoned.†

This work was done whilst I was at the Department of Aeronautical Engineering, Indian Institute of Science, Bangalore. I am deeply grateful to Professor S. Dhawan, Professor C. V. Joga Rao and all their colleagues for the warm welcome given to me. I am particularly indebted to Mr G. N. Venkataramana Rao, who was in charge of the laboratory in which I worked, and to him, Professor Dhawan, Mr S. P. Parthasarathy and others for many stimulating discussions of the experiments. My gratitude goes also to Mr J. A. Doss, Mr B. Noronha, Mr D. Srinivasaiah and Mr S. Ramachandra Iyer for their skilled assistance with the construction of apparatus. My stay in Bangalore was made possible by the award of a Rutherford Memorial Scholarship by the Royal Society, to which body I also express my deep gratitude, not only for the financial assistance but also for their active interest in my work in India.

REFERENCES

Bowden, K. F. 1962 *J. Geophys. Res.* **67**, 3181.
Bowden, K. F. & Howe, M. R. 1963 *J. Fluid Mech.* **17**, 271.
Clauser, F. H. 1956 *Adv. Appl. Mech.* **4**, 1.
Comte-Bellot, G. 1959 *C. R. Acad. Sci.* **248**, 2710.
Comte-Bellot, G. 1961*a* *C. R. Acad. Sci.* **253**, 2457.
Comte-Bellot, G. 1961*b* *C. R. Acad. Sci.* **253**, 2846.
Davies, P. O. A. L., Fisher, M. J. & Barratt, M. J. 1963 *J. Fluid Mech.* **15**, 337.
Dhawan, S. & Vasudeva, B. R. 1959 *J. Aero. Soc. India*, **11**, 1.
Favre, A. J., Gaviglio, J. J. & Dumas, R. 1957 *J. Fluid Mech.* **2**, 313.
Favre, A. J., Gaviglio, J. J. & Dumas, R. 1958 *J. Fluid Mech.* **3**, 344.
Grant, H. L. 1958 *J. Fluid Mech.* **4**, 149.
Hinze, J. O. 1959 *Turbulence.* New York: McGraw-Hill.
Klebanoff, P. S. 1955 *N.A.C.A. Rept.* no. 1247.
Kline, S. J. & Runstadler, P. W. 1959 *J. Appl. Mech.* **26**, 166.
Laufer, J. 1954 *N.A.C.A. Rept.* no. 1174.
Lilley, G. M. 1963 *Coll. Aero. Cranfield Note*, no. 140.
Lilley, G. M. & Hodgson, T. H. 1960 *Coll. Aero. Cranfield Note*, no. 101.

† In this case, the flow visualization experiments of Kline & Runstadler (1959) seeming to show such an eruption are presumably to be explained by the fact that the dye was injected through the wall; any similar inward motion would not have been seen.

ROTTA, J. C. 1962 *Prog. Aero. Sci.* (Pergamon), **2**, 1.

SCHUBAUER, G. B. & SKRAMSTAD, H. K. 1947 *J. Res. Nat. Bur. Stand.* **38**, 251.

STERNBERG, J. 1962 *J. Fluid Mech.* **13**, 241.

TOWNSEND, A. A. 1951 *Proc. Camb. Phil. Soc.* **47**, 375.

TOWNSEND, A. A. 1956 *The Structure of Turbulent Shear Flow.* Cambridge University Press.

TOWNSEND, A. A. 1957 Paper in *Boundary Layer Research* (ed. H. Görtler), IUTAM symposium Freiburg. Berlin: Springer.

TOWNSEND, A. A. 1961 *J. Fluid Mech.* **11**, 97.

TRITTON, D. J. 1967 *J. Fluid Mech.* **28**, 433.